Statistical properties of radiation power levels from a high-gain free-electron laser at and beyond saturation

C.B. Schroeder, W.M. Fawley, and E. Esarey
Center for Beam Physics, Lawrence Berkeley National Laboratory, Berkeley, CA 94720, USA

We investigate the statistical properties (*e.g.*, shot-to-shot power fluctuations) of the radiation from a high-gain free-electron laser (FEL) operating in the nonlinear regime. We consider the case of an FEL amplifier reaching saturation whose shot-to-shot fluctuations in input radiation power follow a gamma distribution. We analyze the corresponding output power fluctuations at and beyond saturation, including beam energy spread effects, and find that there are well-characterized values of undulator length for which the fluctuations reach a minimum.

1. Introduction

A detailed understanding of the statistical properties of the radiation produced at or near saturation by a high gain FEL based upon self-amplified spontaneous emission (SASE) is critical for generation of FEL radiation in future proposed x-ray devices [1,2]. For example, the ability to describe, predict, and control shot-to-shot (instantaneous and time-averaged) power fluctuations in the output radiation will be important for most user applications.

In this paper, we present numerical results concerning certain statistical properties of the radiation emitted by high-gain FEL's operating in the nonlinear regime at and beyond saturation. Our study is motivated by recent proposals [3,4] to improve the output properties (*e.g.*, reduced spectral bandwidth or pulse duration) of high gain SASE FEL's. The basic scheme is to first use a SASE FEL to generate radiation, which would then be manipulated (by a monochromator or other optics) to serve as the input seed to a second undulator acting as a nearly monochromatic FEL amplifier. Our particular interest is to determine the optimal length for the second undulator to minimize pulse-to-pulse output power fluctuations (which arise naturally from the fluctuations associated with the monochromatized SASE radiation of the first undulator).

2. FEL amplifier in the nonlinear regime

In this section we examine the characteristics of the output radiation as a function of undulator length L_u for various input powers of a *monochromatic* FEL amplifier operating at and beyond saturation. Figure 1 shows the power P versus location along the undulator, as obtained from one-dimensional (1D) simulations (*i.e.*, no diffraction) using the GINGER code [5] to model a monochromatic FEL amplifier with the following physical parameters: wavelength $\lambda_s = 1\,\mu$m, beam current $I_B = 1.0\,$kA, energy $\gamma = 400$, instantaneous energy spread $\sigma_\gamma = 0$, normalized emittance $\varepsilon_N = 20\pi\,$mm-mrad, FEL parameter $\rho = 6.4\times10^{-3}$, and undulator period $\lambda_u = 4.0\,$cm and normalized strength $a_u = 2.65$. The curves in Fig. 1 show the exponential power gain and saturation for three initial input radiation powers, 2.5, 25, and 250 kW, and are nearly self-similar in shape and saturation power (a well-known result for $P_{\rm in} \ll P_{\rm sat}$). Once saturation is reached, the output radiation power then oscillates with L_u at the synchrotron bounce period

$$\tau_b \simeq \frac{\lambda_u}{2c}\left(\frac{1+a_u^2}{a_u\,a_s}\right)^{1/2}, \qquad (1)$$

where a_s is the normalized radiation vector potential. The oscillations have near-perfect periodicity, indicating that most particles are deeply-trapped in the ponderomotive well where the bounce period is nearly constant.

Once L_u exceeds the length necessary to en-

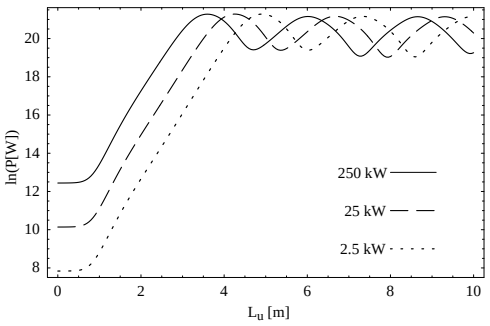

Figure 1. Radiation power $\ln(P[\mathrm{W}])$ versus undulator length L_u for several input powers.

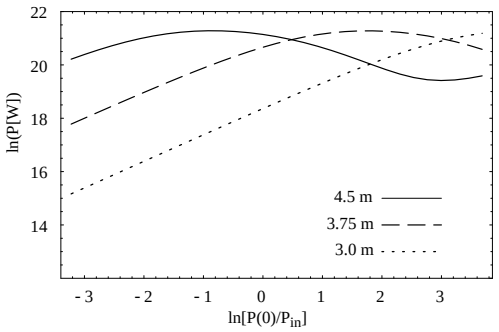

Figure 2. Output power $\ln(P[\mathrm{W}])$ versus input power $P(0)$ (normalized to a nominal input power $P_{\mathrm{in}} = 25$ kW) for several undulator lengths.

ter the saturated gain regime, we expect that the relative shot-to-shot power fluctuations will decrease. This behavior is confirmed by Fig. 2, where we plot the output radiation power as a function of the input radiation power (normalized to a nominal input power $P_{\mathrm{in}} = 25\,\mathrm{kW}$) for several different undulator lengths. If L_u is much shorter (*e.g.*, $L_u = 3\,\mathrm{m}$ with $P_{\mathrm{in}} = 25\,\mathrm{kW}$) than the saturation length corresponding to the first maximum of output radiation power (*e.g.*, $L_{\mathrm{sat}} = 4.25\,\mathrm{m}$; *cf.* dashed curve of Fig. 1), then there is a large variation of output power with input power. As L_u approaches the length necessary for saturation, the sensitivity to input power becomes much less, as shown by the solid curve of Fig. 2. Consequently, we conclude that in the presence of shot-to-shot input power fluctuations, higher stability of the output radiation power can be achieved by making the undulator length of a monochromatic FEL amplifier sufficiently long to operate in the saturated gain regime.

2.1. Monochromatized SASE Fluctuations

As discussed in Sec. 1, one might consider using the monochromatized radiation produced by a SASE FEL to seed a second undulator. For the split undulator/monochromator scheme [3,4], one desires a relatively narrow frequency bandwidth σ_{m} to satisfy user requirements. However, the bandwidth must be large enough to pass sufficient power to the second undulator to greatly exceed the effective e-beam shot noise power. Consequently, one will probably operate the monochromator in the regime $1 \leq M \lesssim 10$, where M is the number of independent longitudinal modes. For $\sigma_{\mathrm{m}} \ll \rho c/\lambda_s$, where $\rho c/\lambda_s$ is the FEL gain bandwidth, the number of modes selected by the monochromator will be $M \sim \sigma_{\mathrm{m}} T$, where T is the pulse duration. For any M, intrinsic fluctuations in the *instantaneous* SASE FEL power in the exponential growth regime follow a negative-exponential probability distribution, characteristic of multimode thermal radiation [6,7]. The fluctuations in the shot-to-shot pulse energy immediately after the monochromator follow a negative-binomial distribution which for a large degeneracy parameter $\langle n\rangle/M \gg 1$, where $\langle n\rangle$ is the mean photon number, reduces to a gamma distribution [6,7]

$$\mathcal{P}(n) = \frac{M^M}{\Gamma(M)} \frac{n^{M-1}}{\langle n\rangle^M} e^{-Mn/\langle n\rangle} , \qquad (2)$$

where $\mathcal{P}(n)$ is the probability density and n the photon number; the corresponding relative root-mean square (RMS) fluctuations are $\sigma_n/\langle n\rangle = 1/\sqrt{M}$.

For the special case of $M = 1$, the instantaneous power within a given radiation pulse is constant (neglecting end effects at the pulse head and tail), and the monochromatic results of the previous section apply to the shot-to-shot fluctuations in instantaneous and time-averaged power. For this case, we can compute the expected RMS fluctuation level of the shot-to-shot

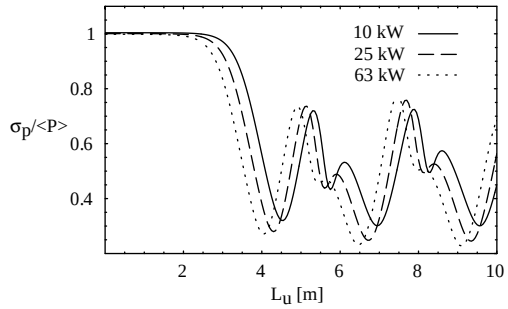

Figure 3. Relative RMS output power fluctuation level $\sigma_P/\langle P\rangle$ versus undulator length L_u for a FEL amplifier whose input power obeys a $(M = 1)$ gamma probability distribution.

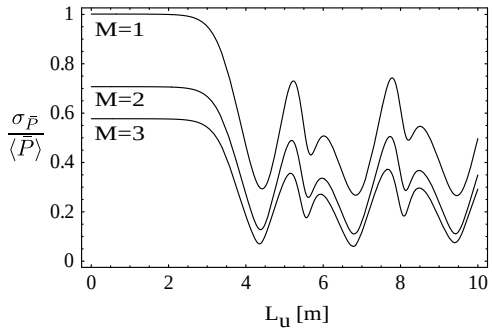

Figure 4. Relative RMS time-averaged output power fluctuation level $\sigma_{\bar{P}}/\langle\bar{P}\rangle$ versus undulator length for $\langle\bar{P}_{\rm in}\rangle = 25$ kW and M =1, 2, and 3.

output power of the second undulator by using an input power probability distribution which follows Eq. (2) with $M = 1$. Figure 3 shows the normalized RMS output power fluctuation $\sigma_P/\langle P\rangle \equiv (\langle P^2\rangle/\langle P\rangle^2 - 1)^{1/2}$ versus L_u for several mean input powers for the 1D example of the previous section. These curves were obtained by using a lookup table of $P_{\rm out}(L_u, P_{\rm in})$ produced by the 1D GINGER runs described previously. For L_u well within the exponential gain regime, $\sigma_P/\langle P\rangle$ remains constant as one would expect since the gain is essentially independent of $P_{\rm in}$. As L_u enters the saturated gain regime, the normalized fluctuation level decreases and becomes nearly periodic, oscillating at the bounce period $c\tau_b$.

For $M \geq 2$, in order to calculate *exactly* the output power $P_{\rm out}(t)$ and various statistical properties such as the ensemble-averaged $\langle P_{\rm out}(t)\rangle$ and RMS fluctuation in average pulse power σ_P, one would have to take into account not only the statistics of the average pulse power as described above, but also the effects of slippage acting upon a time-dependent $P(t)$ for each independent pulse, *i.e.*, calculating an ensemble of full time-dependent simulations. However, in this paper we determine an approximate answer to the statistical problem for $M \geq 2$ which relies upon two simplifications: (1) Following the monochromator, we presume that the temporal coherence length is much larger than the slippage length L_s in the second undulator. For $M \leq 10$ and electron beam pulse lengths $\gtrsim \mathcal{O}(3L_s)$, this will almost certainly be true, and slippage will play a very minor role in pulse evolution. (2) Defining the time-dependent gain $G[z, P_{\rm in}(t)] \equiv P_{\rm out}(t)/P_{\rm in}(t)$, we presume G is well-approximated by the first few terms of a Taylor expansion about the time-averaged input power $\bar{P}_{\rm in}$ corresponding to a given shot. Note that in the exponential gain regime, $\partial G/\partial P_{\rm in} \approx 0$ and the output statistics of the ensemble- and time-averaged output power, $\langle\bar{P}\rangle$, will follow those of $\langle\bar{P}_{\rm in}\rangle$.

To examine the sensitivity of $\langle\bar{P}\rangle$ to the probability distribution (i.e., M), we used the above simplifications to compute the relative RMS shot-to-shot fluctuations in the time-averaged output power, $\sigma_{\bar{P}}/\langle\bar{P}\rangle$, as a function of L_u for several different M with $\langle\bar{P}_{\rm in}\rangle = 25\,$kW. Figure 4 shows that the general curve shape and the undulator lengths where the output time-averaged power fluctuations reach local minima appear quite insensitive to the particular choice of input power probability distribution. The first minimum occurs at the first maximum of the mean output power ($L_{\rm sat} = 4.25$ m), while the second local fluctuation minimum occurs at the minimum of the post-saturation output power, at $L_u = 5.35$ m (*cf.* dashed curve of Fig. 1). Consequently, it does appear that there is an optimal length for the second undulator to minimize the time-averaged output power fluctuations.

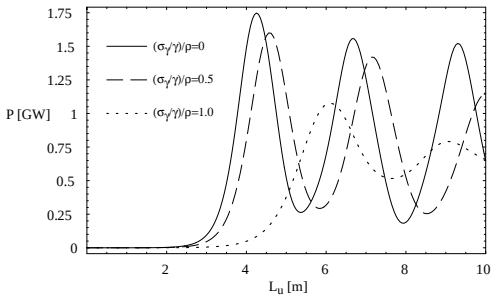

Figure 5. Radiation power P[GW] versus undulator length L_u for several initial energy spreads and an input power $P_{\rm in} = 25$ kW.

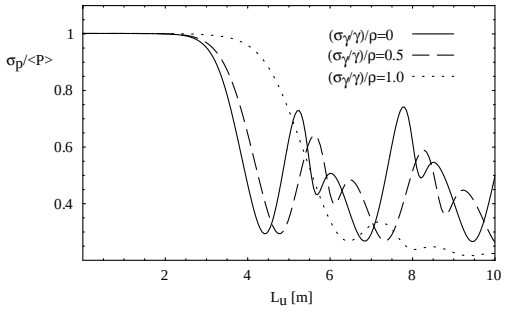

Figure 6. Relative RMS output power fluctuations $\sigma_P/\langle\bar{P}\rangle$ versus undulator length L_u for several initial uncorrelated energy spreads, with $\langle\bar{P}_{\rm in}\rangle = 25$ kW and $M = 1$.

2.2. Effects of beam energy spread

The effects of a non-zero instantaneous energy spread σ_γ on the statistical properties of the radiation were also examined. Figure 5 shows the radiation power versus L_u for initial uncorrelated energy spreads $\sigma_\gamma/(\gamma\rho)$ ranging from zero to one, with input power $P_{\rm in} = 25$ kW. Note that the oscillation amplitude and wavenumber decrease as σ_γ increases, presumably due to a much larger spread in bounce periods associated with completely filled ponderomotive wells.

Non-zero energy spread also strongly affects the shot-to-shot output power fluctuation level. Figure 6 plots $\sigma_P/\langle\bar{P}\rangle$ versus L_u for different initial uncorrelated energy spreads assuming that the time-averaged input power obeys a negative-exponential probability distribution ($M = 1$) and $\langle\bar{P}_{\rm in}\rangle = 25$ kW. One sees that an increase in energy spread σ_γ reduces the output power fluctuation level for large undulator lengths.

3. Conclusions

This paper has investigated the statistical fluctuations of the expected output power from a split undulator/monochromator SASE FEL configuration operating at and beyond saturation. There are well-defined minima in the relative RMS output power fluctuation level for a given input power and energy spread. The locations of the minima are insensitive to the initial fluctuation distribution and correlate strongly with power maxima of post-saturation oscillations. For large electron beam energy spreads [*i.e.*, $\sigma_\gamma/(\gamma\rho) \gtrsim 1$], the natural post-saturation fluctuation level is reduced, but, due to the reduced output power and required increase in undulator length, it is unlikely experiments would purposely operate in this regime.

Acknowledgements

This work was supported by the U.S. Department of Energy under Contract No. DE-AC03-76SF0098. Computational resources were provided in part by the National Energy Research Supercomputer Center (NERSC).

REFERENCES

1. Linac Coherent Light Source (LCLS) Conceptual Design Report, SLAC Report No. SLAC-R-593, UC-414, 2002.
2. TESLA Technical Design Report, DESY Report No. DESY-2001-011, 2001.
3. J. Feldhaus *et al.*, Opt. Commun. 140 (1997) 341.
4. C.B. Schroeder *et al.*, J. Opt. Soc. Am. B 19 (2002) 1782.
5. W.M. Fawley, LBNL Report No. 49625, 2002.
6. E.L. Saldin, E. A. Schneidmiller, M.V. Yurkov, Opt. Commun. 148 (1998) 383.
7. J. Goodman, *Statistical Optics* (Wiley, New York, 1985).